

THE ANALYSIS OF OVERALL SHIP FUEL CONSUMPTION IN ACCELERATION MANOEUVRE USING HULL-PROPELLER-ENGINE INTERACTION PRINCIPLES AND GOVERNOR FEATURES

Hamid Zeraatgar

Amirkabir University of Technology, Department of Maritime Engineering, Tehran, Iran

M. Hossein Ghaemi

Gdańsk University of Technology, Faculty of Ocean Engineering and Ship Technology, Poland

ABSTRACT

The problem of reduction of greenhouse gas emissions in shipping is currently addressed by many research works and related industries. There are many existing and visionary technologies and ideas, which are conceptually defined or practically realised. This goal can be achieved in different ways, and reducing fuel consumption is one of the major methods. In these circumstances, the aim of this study is to analyse the possibility of fuel consumption reduction by using an alternative control strategy for low-speed marine diesel engines which would take into account the interactions between hull, propeller and main engine. For this purpose, a mathematical model including ship hull and propulsion system is developed. A case study is conducted for a ship for which the results of both the ship hull and screw propeller model tests are available. A low-speed two-stroke diesel engine is then selected for the considered ship. Two different governors are included in the model and their parameters are changed to investigate the dynamic behaviour of the system when simulating the forward acceleration mode in calm sea conditions. The research is mainly focused on variations of fuel consumption by the ship passing a certain distance to reach the nominal constant speed. It is concluded that, for a given travel distance, it is possible to save considerable amount of fuel at the expense of slight increase of journey time.

Keywords: Modelling and simulation; fuel consumption; hull-propeller-engine interactions; ship propulsion system; governor; control strategy

NOMENCLATURE

A_s	wetted surface (m ²)	H_s	pitch due to slip (m)
C_{Ts}	total resistance coefficient	J_A	advance number
C_{F0s}	residual frictional resistance coefficient	K_E	engine gain
C_{Rs}	residual resistance coefficient	K_R	controller gain
C_{AA}	air resistance coefficient	K_t	thrust coefficient
δC_F	roughness coefficient	K_q	torque coefficient
CF	total consumed fuel (kg)	L_{WLS}	water line length (m)
D_p	propeller diameter (m)	M	output of the governor
E	error signal	n_E	rate of revolution of engine shaft (rpm)
h	fuel rack or fuel mass flow rate (kg/s)	n_p	rate of revolution of propeller (rps)
H	geometrical pitch (m)	\dot{n}_p	propeller angular acceleration (rad/s ²)
H_A	advance pitch (m)	\bar{n}	commanded angular velocity of the shaft (rad/s)
		n_{ss}	rotational speed of the shaft in steady-state conditions (rad/s)

Q_p	propeller torque (kNm)
Rn_s	Reynolds Number
R_r	total resistance in calm water (kN)
R_{Ts}	total resistance (kN)
S	journey distance (Nm)
t	time, thrust deduction factor
T	thrust (kN)
T_E	time constant of engine response (s)
t_f	final journey time (duration of journey)
T_n	net thrust (kN)
T_{Ri}	time constant of governor
u	surge velocity (m/s)
u_A	advance speed (m/s)
\dot{u}	surge acceleration (m/s ²)
w	wake fraction
$x_{\dot{u}}$	surge added mass (t)
Z_E	number of engine cylinders
η_0	open water propeller efficiency
ω_E	angular velocity of engine shaft (rad/s)
ρ	water density (t/m ³)
τ	engine response delay (s)

INTRODUCTION

In the ship design process, the ship resistance, as well as the propeller and engine performance are traditionally considered in calm water and steady-state conditions, individually. Then, at the end of design, the engine-propeller interaction in calm water conditions is considered for optimum design. However, not only the steady-state conditions, but also the dynamic hull-propeller-engine interactions taken into account in ship design are not real conditions. Several attempts have been made to include the dynamic interactions between the above three elements. This kind of study may lead to better understanding of real conditions of operation of such sub-elements as engine and propeller, which may have an impact on their design. It may also ensure better control of the engine, which may cut the fuel consumption, as well as improve the overall total ship performance and comfort of crew and passengers. The fuel consumption reduction means decreasing greenhouse gas emissions during ship operation. The purpose of this study is to analyse the possibility of fuel consumption reduction by using an alternative control strategy for low-speed marine diesel engines which would take into account the main interactions between hull, propeller, and main engine.

Schulten [7] considered the interactions between diesel engine, ship and propeller during manoeuvres in calm water. Bondarenko and Kashiwagi [1] studied the dynamic behaviour of a ship propulsion plant in actual seas. They concluded that a conventional governor cannot effectively control the ship propulsion plant in cases of large and abrupt propeller torque losses. This fact suggests the necessity of developing a new control algorithm which could effectively reject disturbances caused by propeller racing.

Theotokatos and Tzelepis [9] have studied the fuel consumption and gas emission generated by a ship engine using a simulation model of hull-propeller-engine interactions. They concluded that the combined engine-propeller-ship modelling can be used for mapping the engine and emission parameters to support the analysis of the propulsion system behaviour over the entire ship operating envelope. The usefulness of mapping of the propulsion system performance and emissions for minimizing the fuel consumption and gaseous emissions during ship operation was evidenced.

Taskar et al. [8] have used a model of engine coupled with a method to estimate wake in waves. They concluded that significant changes in propulsion performance have been observed in the presence of waves as compared to the steady state operation. It has been shown that the engine propeller response i.e. power fluctuations, propeller speed fluctuations, and torque fluctuations can be obtained through a coupled simulation making use of realistic engine and propeller models.

Mizythras et al. [5] have studied the performance of an engine and its elements during acceleration in rough seas using hull-propeller-engine interactions. Their analysis has revealed that the presence of the engine governor limiters and their application timing affect the overall ship's performance.

The hull-propeller-engine interaction simulation seems to be inevitably the future of ship dynamics simulations for assessing all aspects of performance of ship's sub-systems and the ship as a whole. However, there are numerous research issues which need to be addressed.

This paper deals with calculation of fuel consumption as an objective function taking into account the hull-propeller-engine interactions in calm water conditions when the ship accelerates from an arbitrary steady-state speed to the steady service speed. For this purpose, a mathematical model of ship hull and propulsion system is developed. A case study is conducted for a ship for which the results of both the ship hull and screw propeller model tests are available. A low-speed two-stroke diesel engine is then selected for the considered ship. Two different governors are included in the model and their parameters are changed to investigate the dynamic behaviour of the system when simulating the forward acceleration mode in calm sea conditions. The research is mainly focused on fuel consumption variation when the ship passes a certain distance to reach the nominal constant speed. It is concluded that, for a given travel distance, it is possible to save considerable amount of fuel at the expense of slight increase of journey time.

HULL-PROPELLER-ENGINE INTERACTIONS IN ACCELERATION MODE

The steady state for a ship is achieved when the hull, propeller, and engines operate in steady-state conditions. In this case, their variable parameters are well-matched and do not change in time. As soon as one of these three components operates in acceleration mode, the others are also forced

to work under changing conditions. The dynamics of each individual component affects other components. At the beginning of the acceleration mode, the ship is operated at low speed in steady-state conditions. The engine and the propeller also work steadily. Then, the full-ahead command is ordered and executed.

PRINCIPLES OF HULL DRAG FORCE MODELLING IN ACCELERATION MODE

Resistance at ship's steady speed

When designing a ship, the hull drag is typically considered for steady speed, straight path, and calm water conditions. However, several dynamic conditions may also be taken into account in simulations making use of a quasi-static model.

The hull resistance of the ship sailing along a straight path in calm water can be estimated using a regressive/empirical formula, a numerical method, and/or from model tests. The first two methods are usually employed in an early stage of ship design, while model testing is utilized at the final stage. The main equations are as follows:

$$R_{T_s} = \frac{1}{2} \rho_s C_{T_s} u^2 A_s \quad (1)$$

$$C_{T_s} = C_{Fos} + C_{R_s} + C_{AA} + \delta C_F \quad (2)$$

$$C_{Fos} = \frac{0.075}{(\text{Log}_{10} \text{Rn}_s - 2)^2} \quad (3)$$

$$\text{Rn}_s = \frac{u L_{WLS}}{\nu_s} \quad (4)$$

$$C_{R_s} = C_{Rm} \quad (5)$$

where u is the ship's surge velocity, and C_{T_s} , C_{Fos} , C_{R_s} , C_{AA} and δC_F are the ship's total, frictional, residual, air, and roughness resistance coefficients, respectively. R_{T_s} is the ship's total resistance, Rn_s is the Reynolds Number, L_{WLS} is the ship's length at the water line level, and A_s is the ship's wetted surface. The residual ship resistance coefficient is equal to the model coefficient obtained from model tests.

Resistance at acceleration

Having known the steady-state hull resistance, the total resistance is estimated by adding the surge added mass force term as follows:

$$R_t = R_{T_s}(u) + x_{ii} \dot{u} \quad (6)$$

where $R_{T_s}(u)$ stands for the steady-state hull resistance as function of its surge speed, u , and $x_{ii} \dot{u}$ is the surge added mass force, being the product of the surge added mass, x_{ii} , and

surge acceleration, \dot{u} . R_t is the ship's total resistance in calm water. For a given ship, the surge added mass is a function of its breadth-to-length ratio and typically is assumed in the range of 5 to 10 percent of ship mass [4].

PROPELLER PERFORMANCE ALONG STRAIGHT PATH IN CALM WATER

Propeller performance is related to the thrust coefficient, K_T , torque coefficient, K_Q , and propeller efficiency in open water conditions, η_0 . It is presented as a function of advance number, J_A , wake fraction, w , thrust deduction factor, t , and cavitation. Normally, the propeller is designed at an early stage of design using the regression formula from a systematic series. It then has to be tested in: (1) open water conditions, (2) behind hull conditions, and (3) in the cavitation tunnel at the final stage of design. The propeller design condition is solely the calm water condition. Following the general formula for thrust generation by the propeller in open water and calm water conditions, the thrust delivered by the propeller and the required torque can be determined as:

$$T = K_T \cdot \rho \cdot n_p^2 \cdot D_p^4 \quad (6)$$

$$Q_p = K_Q \cdot \rho \cdot n_p^2 \cdot D_p^5 \quad (7)$$

where:

$$K_T = f_1(J_A) = f_1(u_A, n_p) \quad (8)$$

$$K_Q = f_2(J_A) = f_2(u_A, n_p) \quad (9)$$

$$J_A = \frac{u_A}{n_p \cdot D_p} = \frac{n_p(H - H_s)}{n_p \cdot D_p} = \frac{H - H_s}{D_p} \quad (10)$$

$$H_A = H - H_s \quad (11)$$

$$u_A = u(1 - w) \quad (12)$$

$$T_n = T(1 - t) \quad (13)$$

$$R_t = T_n \quad (14)$$

In these formulas, T_n is the net thrust, T is the thrust, Q_p is the propeller torque, H is the geometrical pitch, H_s is the pitch due to slip, and H_A is the advance pitch. ρ is water density, n_p is the rate of revolution of the propeller shaft (in revolutions per second), and D_p is the propeller diameter.

Under the acceleration mode the surge speed, u , varies in time, as a result of which the advance speed, u_A , and the propeller speed also change. Thus, the advance ratio J_A changes nonlinearly. Additionally, the wake fraction and the thrust deduction coefficient also vary. Therefore:

$$J_A(t) = \frac{u_A(t)}{D_p \cdot n_p(t)} \quad (15)$$

$$T(t) = K_t (J_A(t)) \cdot \rho \cdot n_p(t)^2 \cdot D_p^4 \quad (16)$$

Here, the same propeller hydrodynamic coefficients from an open water propeller test are applied, even if the instantaneous kinematic variables are employed. In order to calculate the propeller thrust, the instantaneous value of $J_A(t)$ is to be calculated based on $n_p(t)$ and $u_A(t)$. The advance speed is related to the wake fraction which is calculated/measured in steady-state conditions at certain ship and propeller speeds.

$$u_A(t) = u(t)(1 - w(t)) \quad (17)$$

To the authors' best knowledge, there is no research addressing the wake fraction $w(t)$ in the acceleration mode. Therefore, its value is assumed equal to that of the ship service speed in steady-state conditions, which is either estimated by the regression formula or taken from the model test results for the ship under consideration. The following empirical formulae may be applied:

$$\begin{aligned} w &= -0.05 + 0.5 \cdot C_B \text{ (Taylor)} \\ w &= 0.7 \cdot C_p - 0.18 \text{ (Heckscher)} \\ w &= 0.45 \cdot C_p - 0.05 \text{ (Robertson)} \end{aligned} \quad (18)$$

The same conditions and assumptions are employed when estimating the thrust deduction factor from the regression formula:

$$t = 0.5 \cdot C_p - 0.12 \text{ (Hecker)} \quad (19)$$

As far as the propeller torque required in the acceleration mode is concerned, an additional torque due to added moment of inertia of propeller, J_{added} , must be counteracted by the engine torque:

$$K_q (J_A(t)) \cdot \rho \cdot n_p(t)^2 \cdot D_p^5 + J_{added} \cdot \dot{n}_p(t) \quad (20)$$

where \dot{n}_p is the propeller rotational acceleration in rad/s².

The propeller surge added mass force, m_{ap} , is approximated as:

$$m_{ap} = K_{ap} \cdot m_p \quad (21)$$

where $K_{ap} = 0.10$ to 0.20 (Veritec, 1985) and m_p is the propeller mass.

The propeller moment of inertia is calculated as:

$$J_p = \frac{D_p^2}{K_p} \cdot m_p \quad (22)$$

where K_p takes values between 19 and 28, with 23 as the typically cited value.

The propeller added moment of inertia can be modelled using a simple method:

$$J_{added} = K_a \cdot J_p \quad (23)$$

where the suggested value of K_a is in the range from 0.25 to 0.30 (Saunders, [6]) or from 0.25 to 0.50 (Veritec, [10]).

An alternative method is the regression method by Macpherson et al. (2007):

$$\begin{cases} J_a = C_{IE} \cdot \rho \cdot D_p^5 \\ C_{IE} = C_1 \cdot EAR \cdot \frac{H}{D_p} - C_2 \end{cases} \quad (24)$$

where EAR is the expanded area ratio.

Tab. 1. Coefficients and (MacPherson et al. [4])

No. of blades (Z_p)	$Z_p=3$	$Z_p=4$	$Z_p=5$	$Z_p=6$
C_1	0.00477	0.00394	0.00359	0.00344
C_2	0.00093	0.0087	0.00080	0.00076

DIESEL ENGINE PERFORMANCE

The diesel engine is modelled using the most simplified mathematical model having the form of the first-order transfer function with delayed response [2]:

$$\frac{Q_E(s)}{h(s)} = e^{-\tau \cdot s} \cdot \frac{K_E}{1 + T_E \cdot s} \quad (25)$$

where h is the fuel rack or fuel mass flow rate [kg/s], τ is the response delay [s], K_E is the gain, and T_E is the time constant [s]. These quantities can be calculated as follows:

$$\tau = \frac{1}{2} \cdot \frac{2 \cdot \pi}{Z_E \cdot \omega_E} = \frac{\pi}{Z_E \cdot 2 \cdot \pi \cdot n_E} = \frac{1}{2 \cdot Z_E \cdot n_E} \quad (26)$$

$$T_E \approx 0,9 \cdot \frac{2 \cdot \pi}{\omega_E} \quad (27)$$

$$K_s = \frac{Q_E(n_{E0})}{h(n_{E0})} \quad (28)$$

where Z_E stands for the number of engine cylinders, and ω_E and n_E represent the angular velocity [rad/s] and the rate of engine shaft revolutions [rpm], respectively. Subscript '0' refers to steady-state conditions at nominal point, e.g. Normal Continuous Rating (NCR). A detailed diesel engine model can be found in (Ghaemi [3]).

The engine is assumed to be equipped with a governor which keeps the shaft rotational speed at a constant level with respect to the operating point of the engine (see Fig. 1).

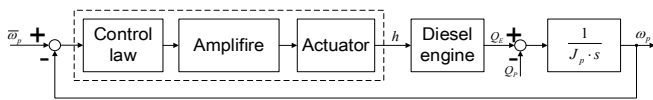


Fig. 1. Simplified engine-propeller block diagram.

If an electrical sensor of angular velocity is applied (for example a small generator), then the transfer function of this element may be represented by 1, due to a relatively small time constant in comparison with other elements.

A governor of PI-action is selected and defined as below:

$$G_R(s) = \frac{M(s)}{E(s)} = K_R \left(1 + \frac{1}{T_{Ri} \cdot s} \right) \quad (29)$$

where K_E and T_{Ri} are the gain constant and the time constant, respectively. $M(s)$ is the output of the governor and $E(s)$ is the error signal, defined as the difference between the commanded rotational speed and the actual one. In the time domain, the above relationship can be written as follows:

$$m(t) = K_p \cdot (\bar{n}(t) - n(t)) + K_i \cdot \int (\bar{n}(t) - n(t)) dt \quad (30)$$

where $\bar{n}(t)$ is the commanded rotational speed of the shaft.

The fuel index change, ΔX_f , can be calculated as follows:

$$\Delta X_f(t) = \frac{m(t)}{n_{ss}} \quad (31)$$

where n_{ss} stands for the rotational speed of the shaft in steady-state conditions with respect to the current operating point, OP:

$$OP = \frac{P_B}{P_{BNCR}} \quad (32)$$

The fuel index at the current operating point should be changed by the increment $\Delta X_f(t)$ of the steady-state index X_{fss} :

$$X_f(t) = X_{fss} + \Delta X_f(t) \quad (33)$$

Finally, the fuel rate (FR) is calculated as:

$$FR(t) = X_f(t) \cdot FR_{NCR} \quad (34)$$

HULL-PROPELLER-DIESEL ENGINE INTERACTIONS AT ACCELERATION MODE IN STRAIGHT PATH AND CALM WATER CONDITIONS

Interactions between hull, propeller and diesel engine occur during ship acceleration and stopping manoeuvres. The general relationship can be formulated as follows:

$$\begin{cases} -R_t(t) + T_n(t) = (\Delta + x_{ii}) \dot{u}(t) \\ Q_E(t) - Q_P(t) = J_p \cdot \dot{\omega}_p(t) \\ T_E \dot{Q}_E(t - \tau) + Q_E(t - \tau) = X_f(t) \\ X_f(t) = X_{fss} + \frac{K_p \cdot (\bar{n}_E(t) - n_E(t)) + K_i \cdot \int (\bar{n}_E(t) - n_E(t)) dt}{n_{ss}} \end{cases} \quad (35)$$

where $n = n_E = n_P$.

For a given fuel injection scenario, the total amount of the consumed fuel, CF , and the journey distance, S , are as follows:

$$CF = \int_0^{t_f} FR(t) dt \quad (36)$$

$$S = \int_0^{t_f} u(t) dt \quad (37)$$

where t_f is the final time and can be an unknown value conditioned by the selected maximum distance. The above equations are to be solved numerically in the time domain.

CASE STUDY, SIMULATION AND RESULTS

For simulation purposes, a computer code is developed based on the delivered model using MATLAB-SIMULINK R2017a. The simulation model is applied to a ship whose hull model was tested for identifying the ship's resistance and whose propeller was tested in model scale. The ship is equipped with a two stroke low-speed diesel engine selected to match the required power, considering the open water and the relative rotative efficiency of the propeller, the hull and shaft efficiencies, and the mechanical efficiency, as well as the sea and engine margins.

SHIP AND ITS PROPULSION SYSTEM

To calculate the performance and perform simulations, a typical vessel, which is a Series 60 ship with block coefficient of 0.60, has been selected. The ship specification is given in Tab. 2. A model of this ship, of 4.58 meters in length, was fabricated, and standard resistance tests were conducted in

NIMALA (National Iranian Marine Laboratory). The model test results extrapolated for the ship are given in Tab. 3.

A B-Wageningen type propeller was selected to propel the ship as specified in Tab. 4. It was tested in open water conditions using the model of 25 cm in diameter. The open water characteristics are shown in Fig. 2.

The prime mover is a MAN-B&W 8S65ME-C8.5 low-speed diesel engine. The Service Maximum Continuous Rating (SMCR) is set for 19433 kW at 92.8 RPM. The steady-state performance of the engine is given in Tab. 5 and illustrated in Fig. 3.

Tab. 2. Ship specifications

No.	Ship parameter	Symbol	Value
1	Displacement	Δ	26980.220 [ton]
		∇	26245.350 [m ³]
2	Wetted length Length BP	L_{WL}	186.260 [m]
		L_{BP}	182.880 [m]
3	Beam	B	24.414 [m]
4	Draught	T	9.782 [m]
5	Ship speed	u	23.82 [Kn]
6	Block coefficient	C_B	0.600 [-]
7	Prismatic coefficient	C_p	0.615 [-]
8	Wetted surface	A	5762.200 [m ²]

Tab. 3. Ship resistance

No.	u [m/s]	F_n	C_t	R_t [kN]	Status
1	0.000	0.00	0.00000	0.000	A
2	1.000	0.023	0.0017700	5.260	A
3	2.000	0.047	0.0017700	21.040	A
4	3.000	0.070	0.0017700	47.340	A
5	4.00	0.094	0.0017760	84.170	A
6	5.13	0.120	0.0017760	138.430	M
7	5.984	0.140	0.0018060	191.526	M
8	6.839	0.160	0.0018070	250.361	M
9	7.694	0.180	0.0018060	316.960	M
10	8.549	0.200	0.0018297	396.061	M
11	9.404	0.220	0.0019500	510.911	M
12	10.259	0.240	0.0019619	611.559	M
13	10.686	0.250	0.0020545	694.845	M
14	11.114	0.260	0.0024144	883.286	M
15	11.969	0.280	0.0030059	1275.386	M
16	12.396	0.290	0.0033275	1514.372	M
17	12.824	0.300	0.0021962	1683.439	M
18	13.679	0.320	0.0035106	1945.546	M

A: Approximated

M: Model test

Tab. 4. Propeller specifications

Type	B-Wageningen Fixed pitch propeller
Diameter	7.590 [m]
Number of blades	5
Area ratio	0.5808
Pitch ratio	1.00 (at full pitch)

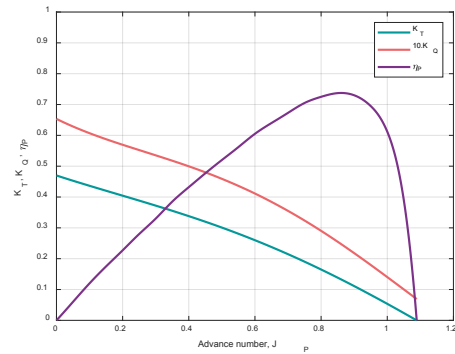


Fig. 2. Open water model test results for the propeller from Tab. 4 (NIMALA)

Tab. 5. Engine performance

Load	Power	Speed	SFOC	FR	Engine eff.
OP [%]	[kW]	[RPM]	[g/kWh]	[kg/s]	[-]
10	1943	43.1	188.0	0.101468	0.4485
15	2915	49.3	178.0	0.144131	0.4736
20	3887	54.3	174.0	0.187872	0.4845
25	4858	58.5	172.0	0.232104	0.4902
30	5830	62.1	170.0	0.275306	0.4959
35	6802	65.4	169.0	0.319316	0.4989
40	7773	68.4	167.5	0.36166	0.5033
45	8745	71.1	166.1	0.403485	0.5076
50	9717	73.7	164.9	0.445093	0.5113
55	10688	76.0	163.7	0.486007	0.5150
60	11660	78.3	162.6	0.526643	0.5185
65	12631	80.4	161.7	0.567342	0.5214
70	13603	82.4	161.1	0.608734	0.5233
75	14575	84.3	161.3	0.653041	0.5227
80	15546	86.1	161.7	0.698275	0.5214
85	16518	87.9	162.3	0.744687	0.5195
90	17490	89.6	163.1	0.792394	0.5169
95	18461	91.2	164.2	0.842027	0.5135
100	19433	92.8	165.5	0.893378	0.5094

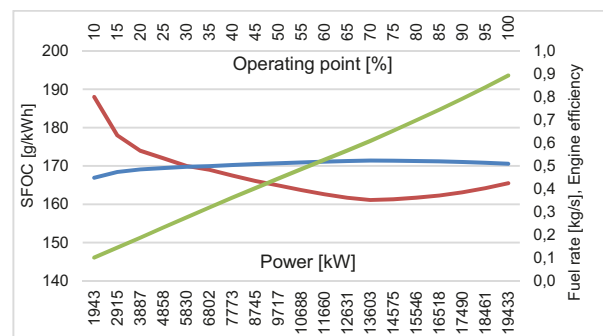


Fig. 3. Steady-state performance of MAN-B&W 8S65ME-C8.5

THE RESULTS

The simulations have been performed under the following assumptions:

1. The shaft, relative-rotative, and gearbox efficiencies are assumed constant and independent of operating conditions. Their exact values are equal to 0.98, 1.00 and 1.00, respectively.
2. The dynamic response of the engine to the torque variation due to fuel rate change is simplified and modelled by a first-order transfer function with time delay. Other engine characteristics involving thermal efficiency are taken from the steady-state engine performance, given in Fig. 3 (quasi-steady analysis).
3. The Normal Continuous Rating (NCR) is supposed to be the same as SMCR.
4. The fuel supply equipment (including fuel pump) is modelled based on the steady-state response. The dynamic behaviour of this equipment is not taken into account.
5. Generally, the governor is of PI-action type.
6. No limiter is applied in the governor, i.e. the governor output is not restricted by the permissible torque or scavenging pressure in the cylinders.
7. Based on the engine specifications provided by the engine manufacturer, the engine always operates above 70% of the NCR rotational speed.
8. The simulation time duration is fixed for a certain journey distance, the length of which is set equal to 15 km.

The overall schematic diagram of the simulation model is presented in Fig. 4.

The model was simulated first for NCR operation to check the steady-state values of selected variables. After approaching a proper set-up of the steady-state hull, propeller, and engine interactions, their results were regarded as initial values for the further unsteady-state analysis. Next, the model was tested for the “full ahead from zero – full stop – full ahead from zero” scenario to check its range of validity. The results of these tests provided positive verification of the model.

After that, a simulation which reflects the real conditions at the acceleration from 70% to 100% of shaft rotational speed (at NCR) was conducted. This is equivalent to the engine power change from 29% to 100% of NCR. Basically, due to turbocharger inefficiency, when the operating point drops below 29% of NCR, the ship propelling becomes ineffective. Therefore, this simulation covered the full acceleration range of the propeller, which is also equivalent to full acceleration range of ship hull.

The simulations aimed at analysing the influence of the governor and its parameters on fuel consumption in the acceleration mode. For the first run, the governor parameters were adjusted using the Ziegler-Nichols method. Next, the simulations were repeated for two cases:

- **Case1:** The P-action governor gain varies from 1 to 27 (higher values make the control system unstable).
- **Case 2:** The proportional gain of the PI-action governor is adjusted and fixed for optimum, while the value of the integral gain varies from 1 to 23 (higher values cause control system instability). The optimum value of the proportional gain is determined equal to 12.15.

All of these simulations start from steady-state conditions at 70% of propeller rotational speed in relation to NCR. The system operation at this initial operating point is continued for 100 seconds to make sure that the variables have become steady. The simulations continue until the 15-km travel distance from the starting point is reached. The ship is sailing along a straight path in calm water conditions. Selected results of these simulations are shown in Figs. 5 to 13. They show the time-histories of engine, propeller, and hull dynamics at optimum governor gains, i.e. the proportional gain equal to 12.15 and the integral gain equal to 2.59 – according to the Ziegler-Nichols method. As shown in Fig. 5, when the fuel rack is changed, the rotational speeds of engine shaft and propeller start with very high acceleration. Their time-histories have one or two fluctuation peaks and in relatively very short time reach approximately the steady-state values. Fig. 6 shows the time-history of fuel consumption.

The slope of the curve is reduced and fixed at a certain level after passing the transient state. This can be illustrated by fuel index or fuel rate variations, the latter shown in Fig. 7. During the first few seconds, the governor, which tries to maintain the rotational speed of the propeller at a constant desired level, changes the rate of the fuel delivered to the engine in a fluctuating manner. These early fluctuations are commanded by the integral part of the governor. The travelled distance and speed of the ship are depicted in Figs. 8 and 9, respectively. The time-history of the distance travelled by the ship has two different slopes. The first slope, which starts from zero and ends at second 100, represents the steady-state motion. The second slope starts from second 100, which is the beginning of the acceleration mode. Initially, the ship has the speed of 8.997 m/s, and then accelerates to reach the final steady-state speed of 11.743 m/s at second 510 (considering the maximum permissible fluctuations at the level of 1% as a criterion to determine the settling time).

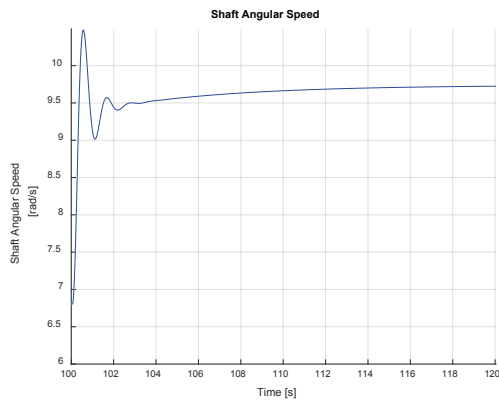


Fig. 5. Time-history of shaft angular speed

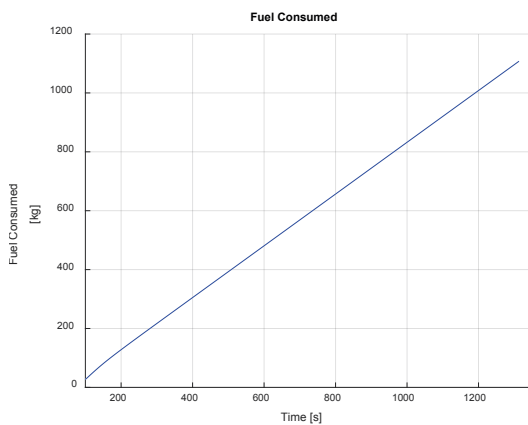


Fig. 6. Time-history of fuel consumption

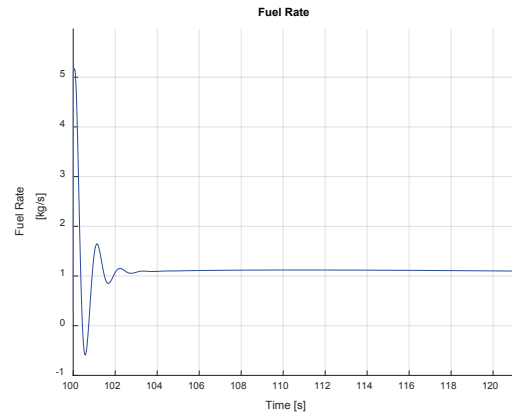


Fig. 7. Time-history of fuel rate

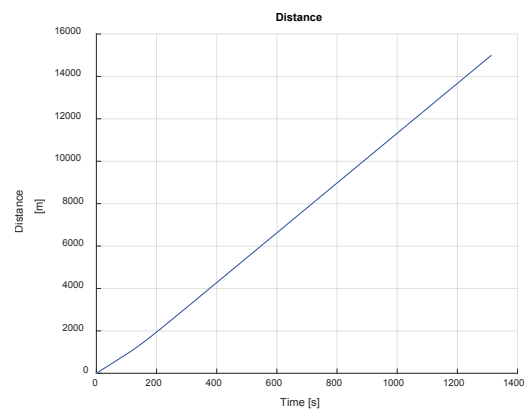


Fig. 8. Time-history of distance travelled by ship

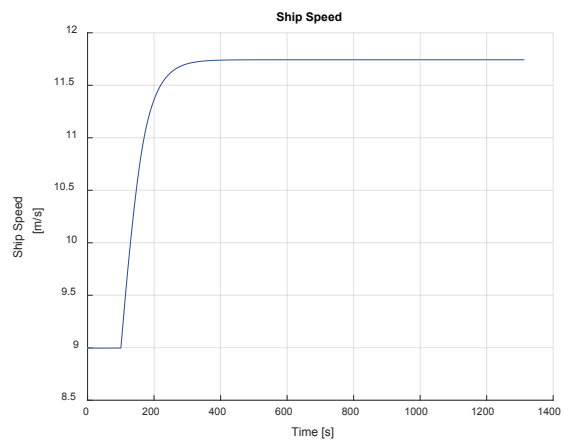


Fig. 9. Time-history of ship speed.

ANALYSIS

The above results show that the propeller and the engine need several tens of seconds to reach the steady-state mode, while the ship needs a several hundreds of seconds to come to the steady state. This is because of very high ship inertia,

compared to the engine shaft and the propeller. This issue becomes clearer when comparing the thrust generated by the propeller with ship's resistance and the torque required by the propeller with that generated by the diesel engine.

For this purpose, Fig. 10 and Fig. 11 compare the thrust-resistance time-histories and the engine torque-propeller torque time-histories, respectively. It can be clearly seen that large inertia of the ship makes that the difference between the current thrust generated by the propeller and the current ship's resistance is significant and a relatively a long time is required to reduce this difference. During this transient time, more thrust is generated than required. Similarly, the difference between the torque delivered by the engine and that required by the propeller is large. However, the time required for reducing this difference is shorter. If the power delivered by the engine (torque multiplied by the angular velocity) is compared with that required by the propeller (advance speed multiplied by the net thrust), it is visible that a relatively very long time is needed to reach the steady-state mode when these two variables are equal and matched. During this time, the supplied fuel could be decreased to adjust the "generated" power against the "required" power, see Fig.12.

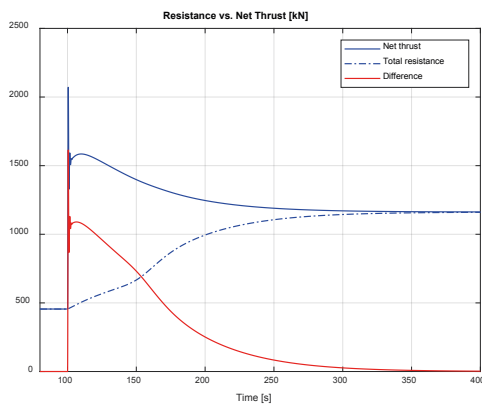


Fig. 10. Comparing time-histories of ship resistance and net thrust generated by propeller

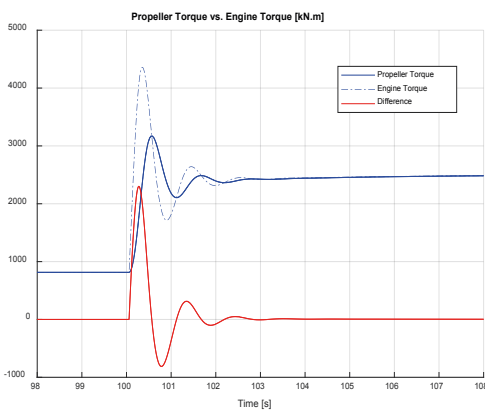


Fig. 11. Comparing time-histories of torque generated by engine and required by propeller

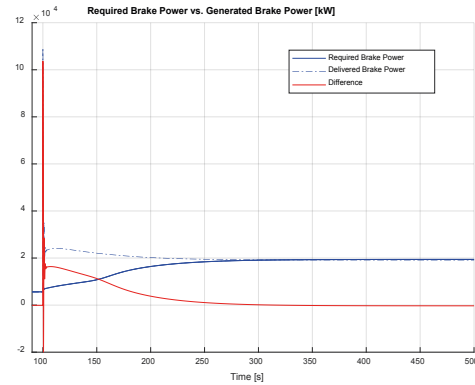


Fig. 12. Comparing time-histories of required and delivered power

Since the main goal of this study was investigating the role of the governor in fuel consumption at the acceleration mode, the governor parameters were assumed to vary from the minimum to the maximum permissible values, taking into account the stability of the control system. Therefore, combinations of "P" and "I" gains were assumed in the electronic governor, and the fuel consumption was analysed for these cases. In order to extract the effect of each of these two parameters, they were changed individually. It means that when the PI-action governor was applied, the proportional gain was kept constant and equal to the optimum value calculated based on the Ziegler-Nichols method. The governor gains, the time required by the ship to approach the 15-km distance, and the corresponding fuel consumption are given in Tab. 6.

As far as the proportional gain is concerned, Tab. 7 shows that a high gain value results in high fuel consumption, while a low gain yields low fuel consumption. Additionally, to achieve a relative 2.7% reduction of the travelling time, 11.5% more fuel is to be combusted. On the other hand, when the integral gain is changed, neither the travelling time nor the consumed fuel is visibly affected.

CONCLUSIONS

The study was focused on green shipping by fuel consumption reduction and included the interactions between hull, propeller and main engine.

Tab.6. Influence of governor integral gain on fuel consumption

Case II: PI-action governor ($K_p=12.15$)		
Governor integral gain K_i	Total time [s]	Total fuel consumption [kg]
1	1213.3	1081.419
2	1213.2	1081.221
3	1213.2	1081.153
4	1213.2	1081.119
5	1213.2	1081.099
6	1213.2	1081.087
7	1213.2	1081.078

Case II: PI-action governor ($K_p=12.15$)		
Governor integral gain K_i	Total time [s]	Total fuel consumption [kg]
8	1213.2	1081.072
9	1213.2	1081.068
10	1213.2	1081.065
11	1213.2	1081.063
12	1213.2	1081.062
13	1213.2	1081.061
14	1213.2	1081.060
15	1213.2	1081.060
16	1213.2	1081.060
17	1213.2	1081.061
18	1213.2	1081.061
19	1213.2	1081.062
20	1213.1	1081.061
21	1213.1	1081.060
22	1213.1	1081.056
23	1213.1	1081.042

Tab.7. Influence of governor proportional gain on fuel consumption

Case I: P-action governor		
Governor proportional gain K_p	Total time [s]	Total fuel consumption [kg]
1	1247.1	964.515
2	1230.8	1019.416
3	1225.2	1038.643
4	1222.3	1048.540
5	1220.6	1054.614
6	1219.4	1058.738
7	1218.5	1061.730
8	1217.9	1064.002
9	1217.4	1065.790
10	1217.0	1067.235
11	1216.6	1068.427
12	1216.4	1069.428
13	1216.1	1070.281
14	1215.9	1071.017
15	1215.7	1071.658
16	1215.6	1072.222
17	1215.4	1072.723
18	1215.3	1073.170
19	1215.2	1073.572
20	1215.1	1073.935
21	1215.0	1074.265
22	1214.9	1074.567
23	1214.9	1074.842
24	1214.8	1075.095
25	1214.7	1075.320
26	1214.2	1074.745
27	1214.2	1075.862

A mathematical model was developed, and the simulations were carried out for the selected case study. The objective of the simulations was investigating the amounts of fuel consumed by the ship in different scenarios to reach the nominal constant speed, when passing a certain distance.

The results have shown that the integral part of the governor has negligible influence on the amount of fuel consumed by the ship. On the other hand, the impact of the gain value of the proportional part on this variable is significant. The results also present the time needed for the ship to pass the distance of 15 km in the forward calm water acceleration mode after reaching the initial steady-state condition at second 100 (until this time the ship passes approximately 1 km). By changing the governor gain from 1 to 27 (the maximum value due to stability) the total time is changed from 1247 s to 1214 s., i.e. a small difference equal to 33 s is observed. However, the time needed for ship speed stabilisation varies from 582 to 1336 s., and this difference is relatively large (the same refers to the shaft rotational speed). The total fuel consumption varies from 964.515 kg (for $K_p = 1$) to 1075.862 kg (for $K_p = 27$), which means the difference by 111.347 kg. Based on these outcomes, it can be concluded that to save 33 s of total time (which is 2.7% of the minimum calculated time for $K_p = 27$), the ship has to combust 111.347 kg more fuel (which is 11.5% more than the minimum calculated fuel consumption for $K_p = 1$).

That means that an attempt to keep the rotational speed as constant as possible by a conventional governor leads to a relatively significant increase of fuel consumption without any considerable influence on the travelling time. Therefore, one way to decrease the fuel consumption as a main criterion for green ship concept is to control ship acceleration. This study has demonstrated the effect of ship acceleration on fuel consumption. Indeed, situations in which the ship accelerates when sailing along a straight path are typical for ship departure, which is a very small part of ship voyage. However, there are other situations, such as navigation in waves for instance, during which the ship is constantly in acceleration conditions and the reduction of acceleration may considerably reduce the total fuel consumption. It should be added here that some optimisation criteria for a ship performing an acceleration manoeuvre can be found in [12].

REFERENCES

1. Bondarenko O., Kashiwagi M.: Dynamic behaviour of ship propulsion plant in actual seas, Journal of the JIME, Vol. 45, Special Issue, 2010.
2. Domachowski Z., Ghaemi M. H.: Marine control systems (in Polish, Okrętowe układy automatyki), Publication of Gdansk University of Technology, ISBN 9788373481770 837348177X, 2007.
3. Ghaemi M.: Changing the ship propulsion system performances induced by variation in reaction degree of turbocharger turbine, Journal of Polish CIMAC.-Vol. 6., No.1, 2011.
4. Lewandowski E.M., 2004, The Dynamics of marine craft, Manoeuvring and Seakeeping, World Scientific, Vol 22.

5. MacPherson D.M., Puleo V.R., Packard M.B.: Estimation of entrained water added mass properties for vibration analysis, SNAME New England Section, 2007.
6. Mzythras P., Boulougouris E., Theotokatos G.: Numerical study of propulsion system performance during ship acceleration, *Ocean Engineering* 149, 2018.
7. Saunders H.E.: *Hydrodynamics in ship design*, SNAME, 1957.
8. Schulten P.J.M.: The interaction between diesel engines, ship and propellers during manoeuvring, Ph.D. thesis, Delft, 2005.
9. Taskar B., Yum K.K., Steen S., Pedersen E.: The effect of waves on engine-propeller dynamics and propulsion performance of ships, *Ocean Engineering*. 122, 2016.
10. Theotokatos G., Tzelepis V.: A computational study on the performance and emissions parameters mapping of a ship propulsion system, *Journal of Engineering for the Maritime Environment*, 229 (1). pp. 58-76. ISSN 1475-0902, 2015.
11. Veritec: *Vibration control in ships*, ISBN 9788251500906, 1985.
12. Wojnowski W., *Marine Combustion Power Plants (Okrętowe Siłownie spalinowe, in Polish)*, Morski Instytut Rybacki, Gdańsk, 1991.

CONTACT WITH THE AUTHORS

Hamid Zeraatgar

e-mail: hamidz@aut.ac.ir

Amirkabir University of Technology
 Department of Maritime Engineering
 424 Hafez Ave
 Tehran, Iran, 15875-4413
IRAN

M. Hossein Ghaemi

e-mail: ghaemi@pg.edu.pl

Gdańsk University of Technology
 Faculty of Ocean Engineering and Ship Technology
 ul. G. Narutowicza 11/12
 80-233 Gdansk
POLAND